In Vitro Selection of State-Specific Peptide Modulators of G Protein Signaling Using mRNA Display†

William W. Ja and Richard W. Roberts*

Division of Chemistry and Chemical Engineering, California Institute of Technology, Pasadena, California 91125

Received January 22, 2004; Revised Manuscript Received May 16, 2004

ABSTRACT: The G protein regulatory (GPR) motif is a ∼20-residue conserved domain that acts as a guanine dissociation inhibitor (GDI) for $G_{i/o\alpha}$ subunits. Here, we describe the isolation of peptides derived from a GPR consensus sequence using mRNA display selection libraries. Biotinylated $G_{i\alpha1}$, modified at either the N or C terminus, serves as a high-affinity binding target for mRNA-displayed GPR peptides. In vitro selection using mRNA display libraries based on the C terminus of the GPR motif revealed novel peptide sequences with conserved residues. Surprisingly, selected peptides contain mutations to a highly conserved Arg in the GPR motif, previously shown to be crucial for binding and inhibition activities. The dominant peptide from the selection, R6A, and a minimal 9-mer peptide, R6A-1, do not contain Arg residues yet retain high affinity (K_D = 60 and 200 nM, respectively) and specificity for the GDP-bound state of $G_{i\alpha1}$, as measured by surface plasmon resonance. The selected peptides also maintain GDI activity for $G_{i\alpha1}$, inhibiting both the exchange of GDP in GTPγS binding assays and the AlF_4^--stimulated enhancement of intrinsic tryptophan fluorescence. The kinetics of GDI activity, however, are different for the selected peptides and demonstrate biphasic kinetics, suggesting a complex mechanism for inhibition. Like the GPR motif, the R6A and R6A-1 peptides compete with $G_{\beta\gamma}$ subunits for binding to $G_{i\alpha1}$, suggesting their use as activators of $G_{\beta\gamma}$ signaling.

Intracellular heterotrimeric guanine nucleotide-binding proteins (G proteins) mediate signaling from cell-surface receptors (GPCRs)[1] to a wide variety of effectors (*1*, *2*). In the inactive state, $G_{\beta\gamma}$ heterodimers bind tightly to GDP-bound G_α subunits, enhancing coupling to specific GPCRs and exhibiting guanine nucleotide dissociation inhibitor (GDI) activity by preventing GDP release from G_α (*3*). Activation by extracellular agonists causes the GPCR to act as a guanine nucleotide exchange factor (GEF), exchanging GDP with GTP in G_α and initiating signal transduction through G_α-GTP and/or $G_{\beta\gamma}$ subunits. The inherent guanosine triphosphatase (GTPase) activity of G_α returns the protein to the GDP-bound state, resulting in reassociation of $G_{\beta\gamma}$ and termination of signaling. Numerous other regulators of heterotrimeric G proteins acting as GDIs, GEFs, or GAPs (GTPase-activating proteins, which accelerate the GTPase activity of G_α subunits and the termination of signaling) add further complexity to the intricate network of intracellular signaling pathways and the kinetics of G protein signaling (*4*).

Direct modulators of G protein signaling would be useful as molecular tools in studies on the involvement of particular G proteins in specific biochemical pathways, supplementing or replacing traditional genetic techniques. Potent molecules with marked specificity for individual G proteins would potentially act as leads for the development of G protein-directed drugs. Drug discovery targeting G proteins has had limited success because of the broad spectrum of signaling events mediated at the G protein level, as well as the high sequence and structural similarities between G protein classes (*5*, *6*). The ability to quickly assay combinatorial libraries for molecules with desired properties provides the potential to alleviate these difficulties (*7*, *8*).

A selection experiment is an iterative process where a large pool of molecules (e.g., composed of nucleic acids, polypeptides, or synthesized compounds) is sieved for functionality (e.g., binding to a protein target) and active library members are retained. Techniques for peptide or protein selections generally involve the physical association or localization of a polypeptide with its encoding nucleic acid sequence, which allows for the identification of isolated peptides by DNA sequencing. In vitro selection has previously been used to recover high-affinity peptides that bind to rhodopsin and compete with $G_{t\alpha}$ subunits for receptor coupling (*9*). More recently, phage display selections produced several classes of peptides that appear to bind to the same site on $G_{\beta\gamma}$ subunits (*10*). Binding of these peptides to $G_{\beta1\gamma2}$ were subsequently shown to accelerate dissociation from $G_{i\alpha1}$, most likely by inducing a conformational change in $G_{\beta\gamma}$ (*11*).

mRNA display is an in vitro peptide selection technique that gives access to high complexity libraries ($>10^{13}$ unique peptide sequences) in a robust format (*12*, *13*). In mRNA

† This work was supported by grants from the NIH (RO160416) and the Beckman Foundation to R.W.R. W.W.J. was supported in part by a DOD National Defense Science and Engineering Graduate Fellowship. R.W.R. is an Alfred P. Sloan Foundation Research Fellow.

* To whom correspondence should be addressed. Telephone: 626-395-3564. Fax: 626-568-9430. E-mail: rroberts@caltech.edu.

[1] Abbreviations: AGS3, activator of G protein signaling 3; Fmoc, fluorenylmethoxycarbonyl; GAP, GTPase-activating protein; GDI, guanine nucleotide dissociation inhibitor; GEF, guanine nucleotide exchange factor; GoLoco, $G_{\alpha i/o}$-Loco interaction; GPCR, G protein-coupled receptor; GPR, G protein regulatory; GTPγS, guanosine 5′-*O*-(3-thiotriphosphate); HPLC, high-performance liquid chromatography; MALDI−TOF, matrix-assisted laser desorption ionization−time-of-flight; MBP, maltose-binding protein; RT-PCR, reverse-transcription polymerase chain reaction; SPR, surface plasmon resonance.

10.1021/bi0498398 CCC: $27.50
Published on Web 06/19/2004

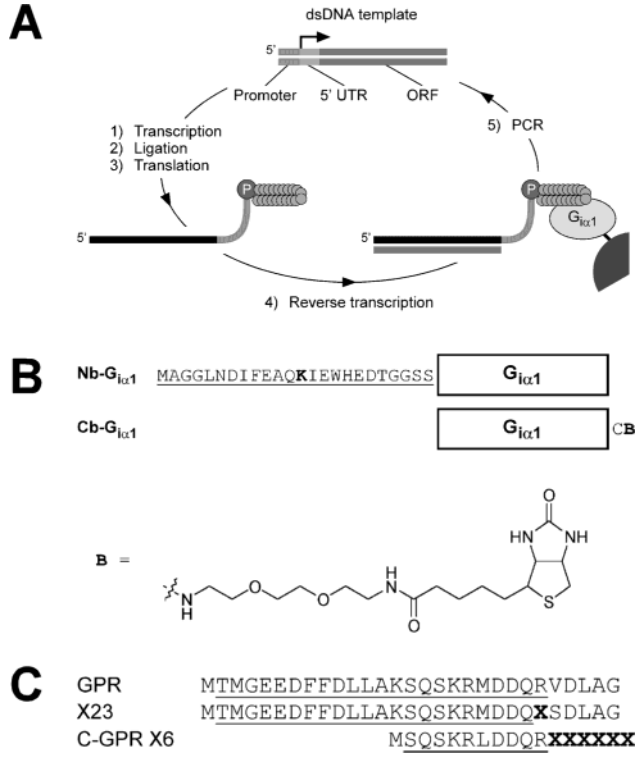

FIGURE 1: (A) In vitro selection scheme using mRNA display. DNA containing a T7 promoter, an untranslated region, and an ORF is transcribed, ligated to a puromycin-DNA linker, and translated to produce a pool of RNA-peptide fusions. Purified fusions are reverse-transcribed prior to selection on an immobilized target ($G_{i\alpha1}$). PCR amplification of the retained cDNA produces the dsDNA template for the next round of selection. (B) Biotinylated $G_{i\alpha1}$ protein constructs. Nb-$G_{i\alpha1}$ is expressed with an N-terminal peptide biotinylation tag (bio-tag, underlined) (*23*, *47*). A specific lysine (bold) in the bio-tag is biotinylated in vivo by biotin holoenzyme synthetase. Cb-$G_{i\alpha1}$ is expressed as a fusion protein with a C-terminal intein. Cleavage and biotinylation of the C terminus of $G_{i\alpha1}$ occur concurrently with the addition of a biotinylated cysteine derivative. (C) Peptides used for mRNA display. A C-terminal constant peptide sequence (QLRNSCA, not shown) results from the required priming site used in PCR amplification of the original DNA templates. **X** represents a random amino acid. Residues from the GPR motif consensus are underlined.

display, an RNA library, produced by in vitro transcription from dsDNA template, is covalently linked to its encoded polypeptide via a 3′-puromycin moiety (Figure 1A). These libraries can be composed of random peptides or mutants of specific sequences, based on the DNA template construction. Pools of RNA-peptide fusions are selected against an immobilized target. Recovered, functional protein sequences are amplified by the reverse-transcription polymerase chain reaction (RT-PCR) to produce an enriched dsDNA pool suitable for the next round of selection.

The G protein regulatory (GPR) or GoLoco motif binds selectively to $G_{i/o\alpha}$ subunits and acts as a GDI, stabilizing the GDP-bound state (*14*−*18*). Single and multiple copies of the ∼20-residue conserved GPR motif are found in a variety of signal-regulating proteins (*19*). Proteins encoding the GPR motif, as well as a synthetic, GPR consensus peptide, compete with $G_{\beta\gamma}$ for binding to G_α subunits (*14*, *15*, *20*), thereby activating $G_{\beta\gamma}$-dependent pathways in the absence of nucleotide exchange (*21*). The high affinity and potency of the GPR motif makes it an ideal scaffold for peptide selection. Here, mRNA display with a GPR-derived library was used to select for novel peptides with high affinity for $G_{i\alpha1}$. The dominant, selected peptide (R6A) was minimized to a 9-residue sequence (R6A-1) that shares identity with only 2 amino acids from the core GPR motif yet retains submicromolar affinity for $G_{i\alpha1}$. The selected peptides retain GDI activity although the kinetics of inhibition differ significantly from that of the GPR consensus. R6A and R6A-1 also maintain the ability to compete with $G_{\beta\gamma}$ subunits for binding to $G_{i\alpha1}$.

EXPERIMENTAL PROCEDURES

Materials. The *Escherichia coli* strains, BL21 and BL21-(DE3), were from Novagen, Inc. (Madison, WI). Restriction enzymes, T4 DNA ligase, and vector pTXB1 were from New England Biolabs, Inc. (Beverly, MA). The G protein expression vector, NpT7-5-H6-TEV-Giα1, was generously provided by Prof. Roger K. Sunahara (University of Michigan). The cDNA clone of human $G_{i\alpha3}$ was obtained from the Guthrie cDNA Resource Center (http://www.cdna.org). The in vivo biotinylation vector, pDW363, was kindly supplied by Dr. David S. Waugh (National Cancer Institute, Frederick, MD). L-[^{35}S]-methionine (1175 Ci/mmol) was purchased from Perkin−Elmer Life Sciences, Inc. (Boston, MA). The polyclonal antiserum BN1, which recognizes the N termini of $G_{\beta1}$ and $G_{\beta2}$, was kindly provided by Prof. Melvin I. Simon. Other reagents were purchased from Sigma−Aldrich Corp. (St. Louis, MO) or VWR International, Inc. (West Chester, PA) unless otherwise stated. DEPC-treated ddH_2O was used for all RNA work. DNA oligos (including the modified oligo, pF30P) were synthesized at the Biopolymer Synthesis and Analysis Facility at the California Institute of Technology. DNA sequencing of generated ORFs on all expression vectors and selected peptide clones was performed at the California Institute of Technology DNA Sequencing Core Facility.

G_α-Subunit Cloning and Expression. Recombinant rat His_6-TEV-$G_{i\alpha1}$ (N-terminal His_6 tag followed by a TEV protease cut site) was expressed and purified essentially as described (*22*). Briefly, *E. coli* BL21(DE3) cells harboring NpT7-5-H6-TEV-Giα1 were grown in 1 L of enriched media [2% (w/v) tryptone, 1% (w/v) yeast extract, 0.5% (w/v) NaCl, 0.2% (v/v) glycerol, and 50 mM KH_2PO_4 at pH 7.2, supplemented with 50 μg/mL ampicillin] to an OD_{600} of 0.5, induced with 0.1 mM IPTG, and collected by centrifugation after ∼6 h of expression at 30 °C. Cells were lysed by French press and purified on Ni-NTA Superflow (Qiagen, Inc., Valencia, CA) using a Pharmacia FPLC system (Amersham Biosciences Corp., Piscataway, NJ). Pure protein fractions were combined and concentrated into HED buffer (50 mM HEPES-KOH at pH 7.5, 1 mM EDTA, and 2 mM DTT) using a Centriprep YM-30 (Millipore Corp., Billerica, MA). The protocol yielded >95% pure protein at ∼20 mg/L culture, and the protein was generally used without removal of the epitope tag.

The ORF of $G_{i\alpha1}$ was PCR-amplified from NpT7-5-H6-TEV-Giα1 with the primers 29.2 (5′-CCA TTC TCG AGC ATG GGC TGC ACA CTG AG) and 35.2 (5′-TCT TGG GAT CCT TAG AAG AGA CCA CAG TCT TTT AG) and ligated into vector pDW363 (*23*) using the *Xho*I and *Bam*HI restriction sites to produce pDW363-Giα1. This vector encodes $G_{i\alpha1}$ with an N-terminal peptide tag that is biotiny-

lated in vivo (Nb-$G_{i\alpha1}$). A 25-mL LB/ampicillin culture (supplemented with 50 μM D-biotin) of *E. coli* BL21 cells harboring pDW363-Giα1 was induced with 1 mM IPTG (at OD_{600} = 0.6), grown at 30 °C for 6 h, and pelleted by centrifugation. Cell pellets were rinsed gently with ddH_2O, snap-frozen in dry ice/ethanol, and stored at −80 °C until needed. Cells were thawed, lysed with B-PER (Pierce Biotechnology, Inc., Rockford, IL), and cleared as per the instructions of the manufacturer. Cleared lysate was applied to a 2-mL monomeric avidin-agarose column (Pierce), washed with 8× 2 mL of 1× PBS/0.1% (v/v) Triton X-100, and eluted with 7× 2 mL of 1× PBS/2 mM D-biotin. The column could be regenerated with 0.1 M glycine at pH 2.8 and reused with negligible loss in binding capacity. Fractions containing Nb-$G_{i\alpha1}$ were combined and concentrated in a Centriprep YM-30 into HGD buffer [50 mM HEPES-KOH at pH 7.5, 10% (v/v) glycerol, and 1 mM DTT] for storage at −80 °C. The 25-mL culture yielded approximately 1 mg of >95% pure Nb-$G_{i\alpha1}$ (~40 mg/L culture).

Nb-$G_{i\alpha3}$ was expressed and purified using the same protocol as for Nb-$G_{i\alpha1}$. The coding region for human $G_{i\alpha3}$ was PCR-amplified from a cDNA clone using primers 30.4 (5′-CCA TTC TCG AGC ATG GGC TGC ACG TTG AGC) and 39.1 (5′-TCT TGG GAT CCT TAA TAA AGT CCA CAT TCC TTT AAG TTG) and ligated into pDW363 using the *Xho*I and *Bam*HI restriction sites. Approximately 150 μg of biotinylated $G_{i\alpha3}$ was obtained from 50 mL of culture (3 mg/L culture), which was sufficient for our experiments. The lower yield of $G_{i\alpha3}$ compared with that of $G_{i\alpha1}$, despite the high-sequence similarity, is consistent with previously published work (*22*).

To produce the C-terminally biotinylated protein, $G_{i\alpha1}$ was expressed as an intein fusion (*24*). The $G_{i\alpha1}$-intein fusion protein was purified via a chitin-binding domain within the intein, which in the presence of thiols undergoes specific self-cleavage, releasing $G_{i\alpha1}$ from the chitin-bound intein. When a biotinylated cysteine derivative is used, cleavage from the intein and biotinylation of $G_{i\alpha1}$ occur in a single step (*25*, *26*). The ORF of rat $G_{i\alpha1}$ was PCR-amplified with primers 33.1 (5′- TTG GTG CCC GCA ACA TAT GGG CTG CAC ACT GAG) and 40.1 (5′- GGT GGT TGC TCT TCC GCA GAA GAG ACC ACA GTC TTT TAG G) and sequentially digested with *Sap*I followed by *Fau*I. Because the coding region of $G_{i\alpha1}$ contains an internal *Sap*I site, aliquots were taken from the initial *Sap*I digest over the course of a 4-min digestion (at 37 °C) and quenched immediately. The aliquots were pooled and desalted (QIAquick PCR purification, Qiagen) followed by a complete *Fau*I digest and agarose gel purification to remove fragments that were cut at the internal *Sap*I site. The *Fau*I/*Sap*I-digested DNA was inserted into pTXB1 at the *Nde*I/*Sap*I restriction sites to create a new ORF encoding a $G_{i\alpha1}$-intein fusion. A 300-mL culture of *E. coli* BL21(DE3) harboring pTXB1-Giα1 was induced at an OD_{600} of 0.6 with 0.5 mM IPTG, grown at 30 °C for 4 h, and collected by centrifugation. Cell pellets were snap-frozen in dry ice/ethanol and stored at −80 °C until needed. Cells were resuspended in lysis buffer (20 mM HEPES-KOH at pH 7.5, 500 mM NaCl, 1 mM EDTA, and 0.1% Triton X-100) and lysed by French press. After the cell debris was cleared by centrifugation (30 min at 12000*g*), 5 mL of chitin beads (New England Biolabs) was added to the supernatant and rotated at 4 °C for 2 h. The beads were collected in a gravity column and washed with 100 mL of column buffer (20 mM HEPES-KOH at pH 7.5, 500 mM NaCl, and 0.1% Triton X-100). To cleave $G_{i\alpha1}$ from the intein and biotinylate the C terminus, the beads were agitated at 4 °C for ~90 h in 5 mL of column buffer containing 1 mM TCEP (Molecular Biosciences, Inc., Boulder, CO) and 0.9 mM *N*,*N*′-D-biotinyl-2,2′-(ethylenedioxy)bis(ethylamine)-L-cysteine (Supporting Information). Sodium 2-mercaptoethanesulfonate was supplemented into the mixture at 20 and 40 h (10 and 30 mM final concentration, respectively). Cb-$G_{i\alpha1}$ was collected with several fractions of column buffer and concentrated using a Centriprep YM-30 into storage buffer (50 mM HEPES-KOH at pH 7.5, 1 mM DTT, 50 μM GDP, 0.1% Triton X-100, and 10% glycerol). Approximately 80% of the protein (>90% purity) is biotinylated (determined by binding to streptavidin agarose), with a yield of ~10 mg/L culture. Higher concentrations of the cysteine derivative result in nearly complete coupling without the need of supplementing 2-mercaptoethanesulfonate, which increases intein cleavage but reduces the percentage of coupled protein (data not shown).

Protein concentrations were determined by UV absorbance at 205 (*27*) or 280 nm using a calculated extinction coefficient (http://paris.chem.yale.edu/extinct.html). Values obtained from either method generally agreed within 5%.

mRNA Display Template Preparation. A DNA template encoding the GPR consensus peptide was constructed from oligos GPR-top (5′-GGG ACA ATT ACT ATT TAC AAT TAC AAT GAC CAT GGG CGA GGA GGA CTT CTT TGA TCT GTT GGC CAA G) and GPR-bot (5′-GCC AGC CAG GTC CAC CCG TTG ATC GTC CAT CCG TTT GGA CTG AGA CTT GGC CAA CAG ATC AAA GAA G). These two oligos were PCR-amplified together with primers 47T7FP (5′-GGA TTC TAA TAC GAC TCA CTA TAG GGA CAA TTA CTA TTT ACA ATT AC) and mycRP (5′-AGC GCA AGA GTT ACG CAG CTG). The X23 library was constructed by stepwise PCR first with oligos GPR-top and 88.2 (5′-AGC GCA AGA GTT ACG CAG CTG GCC AGC CAG GTC AGA DNN TTG ATC GTC CAT CCG TTT GGA CTG AGA CTT GGC CAA CAG ATC AAA GAA G; N = A, C, G, or T; D = A, G, or T) and subsequently with the primers, 47T7FP and mycRP. The C-GPR extension library was generated by PCR amplification of the template C-GPR-X6 (5′-AGC GCA AGA GTT ACG CAG CTG SNN SNN SNN SNN SNN SNN CCG TTG ATC GTC CAG CCG TTT GGA CTG AGA CAT TGT AAT TGT AAA TAG TAA TTG TCC C; S = C or G) with primers 47T7FP and mycRP. The purified (QIAquick PCR purification) dsDNA constructs contained a T7 promoter, an untranslated region, and an ORF containing a 3′ constant sequence encoding the peptide QLRNSCA.

In vitro transcription reactions (80 mM HEPES-KOH at pH 7.5, 2 mM spermidine, 40 mM DTT, 25 mM $MgCl_2$, 4 mM each of ATP, CTP, GTP, and UTP, and ~10 μg/mL DNA template) were treated with RNA*secure* (Ambion, Inc., Austin, TX) prior to initiating the reaction with T7 RNA polymerase (*28*). Transcription reactions were incubated at 37 °C for ~4 h, quenched with 0.1 volume of 0.5 M EDTA, phenol-extracted using Phase Lock Gel (Brinkmann Instruments, Inc., Westbury, NY), and desalted by 2-propanol precipitation. Full-length mRNA was purified by denaturing

urea−PAGE, collected from excised gel pieces by passive diffusion in water, and desalted by ethanol precipitation.

The puromycin-DNA linker, pF30P (5′-dA_{21}[S9]$_2$dAdCdC-P; S = spacer phosphoramidite 9; P = CPG-puromycin; 5′-phosphorylated using phosphorylation reagent II; Glen Research Corp., Sterling, VA) was ligated to mRNA templates using a splint oligo (5′-TTT TTT TTT TTN AGC GCA AGA GT). RNA (10 μM final concentration), splint, and pF30P (1:1.1:0.5, respectively) were hybridized by heating at 95 °C for ∼3 min, adding T4 DNA ligase buffer (1× final concentration), and cooling on ice for 10 min. SUPERase·In (1 unit/μL, Ambion) and T4 DNA ligase (1.6 units/pmol mRNA) were added and the reaction was incubated at room temperature for >2 h. Ligated mRNA-F30P was gel-purified and desalted as described above.

RNA and RNA-F30P concentrations were estimated by their absorbance at 260 nm using the equation: c (pmol/μL) = A_{260}/(10S), where S is the length of the template in kilobases.

mRNA Display. Purified mRNA-F30P templates were translated in rabbit reticulocyte lysate (Red Nova lysate, Novagen) with ^{35}S-methionine labeling under optimized conditions (100 mM KOAc, 0.5 mM MgOAc, 1 unit/μL SUPERase·In, and 0.5 μM mRNA-F30P) and supplemented with unlabeled L-methionine (0.5 mM final concentration). After incubation for 1 h at 30 °C, additional KOAc and $MgCl_2$ were added to 585 and 50 mM (final concentration), respectively. The reactions were then incubated on ice for 15 min to facilitate RNA−peptide fusion formation (*29*). Reactions were used directly or stored at −80 °C until needed. RNA-peptide fusions were purified by dilution into a 100-fold excess of 1× isolation buffer (50 mM HEPES-KOH at pH 7.5, 1 M NaCl, 1 mM EDTA, 1 mM β-mercaptoethanol, and 0.05% (v/v) Tween 20) and ∼100 μL (dry volume) of prewashed oligo dT-cellulose (New England Biolabs). After rotating at 4 °C for 1 h, the oligo dT-cellulose was washed thoroughly with 0.4× isolation buffer in a 0.45-μm centrifuge tube filter (Costar Spin-X, Corning, Inc., Corning, NY). RNA-peptide fusions were eluted with pre-warmed (50 °C) dT-elution buffer (10 mM Tris-HCl at pH 7.5 and 1 mM β-mercaptoethanol). Fusions were 2-propanol-precipitated with linear acrylamide (Ambion) as a carrier and subsequently reverse-transcribed (Superscript II, Invitrogen Corp., Carlsbad, CA) with the oligo, mycRP.

The affinity matrix for selection was prepared by rotating Nb- and/or Cb-$G_{i\alpha1}$ (∼10 μg each) with ∼20 μL streptavidin agarose (Immobilized NeutrAvidin on Agarose, Pierce) in buffer A (20 mM HEPES-KOH at pH 7.5, 200 mM NaCl, 5 mM $MgCl_2$, 1 mM EDTA, and 0.05% Tween 20) at 4 °C for >1 h. The slurry was supplemented with 1 mM D-biotin (∼0.1 mM final concentration) and rotated for an additional 10 min to block biotin-binding sites. After washing thoroughly with buffer A2 [buffer A supplemented with 2 μM GDP, 1 mM β-mercaptoethanol, 0.2% (w/v) BSA, and 1 μg/mL yeast tRNA (Roche Diagnostics Corp., Indianapolis, IN)], reverse-transcribed fusions were rotated with the affinity matrix in 1 mL of buffer A2 at 4 °C for 1 h. The matrix was then washed with 4× 1 mL of buffer A2 followed by 2× 1 mL of buffer A. Bound fusions were eluted with 2× 0.1 mL of 0.15% (w/v) SDS through a 0.45-μm centrifuge tube filter. After the SDS was removed using SDS-OUT (Pierce), cDNA was ethanol-precipitated with linear acrylamide (Ambion). PCR amplification of the cDNA with primers 47T7FP and mycRP produced the dsDNA template for the next round of selection. DNA templates could also be directly cloned (TOPO TA cloning for sequencing kit, Invitrogen) for subsequent DNA sequencing.

For the C-GPR X6 extension library selection, RNA-F30P templates encoding R6A were removed by subtractive hybridization as described previously using the anti-R6A oligo, 25.2 (5′-CAA GTA CTC CCA CCA GTA CAG AAA-biotin) prior to the 7th and 8th rounds of selection (*30*).

Binding assays using RNA-peptide fusions on immobilized protein targets were performed similarly, except that translation reactions were prepared without supplementing with unlabeled L-methionine and washes were often performed using spin filters (0.45-μm, Costar Spin-X). Fusions used for binding assays were also often RNase-treated (RNase, DNase-free, Roche) prior to use.

Peptide Preparation. Peptides were synthesized with amidated C termini on a 432A Synergy peptide synthesizer (Applied Biosystems, Foster City, CA) using standard Fmoc chemistry. After synthesis, peptides were deprotected and cleaved from the resin by agitation in TFA/1,2-ethanediol/thioanisole (90:5:5) for 2 h at room temperature. Peptides were precipitated with methyltertbutyl ether and pelleted by centrifugation. Crude peptides were dissolved in ddH_2O (hydrophobic peptides were dissolved in DMSO prior to being diluted in ddH_2O) and purified by reversed-phase HPLC (C18, 250 × 10 mm, Grace Vydac, Hesperia, CA) to >95% purity on an aqueous acetonitrile/0.1% TFA gradient. Peptide masses were confirmed by MALDI−TOF mass spectrometry. Peptide concentrations were determined by absorbance at 280 nm using a calculated extinction coefficient (http://paris.chem.yale.edu/extinct.html).

The L19 GPR and R6A peptides were also expressed as fusions to maltose-binding protein (MBP) using the in vivo biotinylation system. GPR or R6A dsDNA was PCR-amplified with universal primer 29.4 (5′-TGA AGT CTG GAG TAT TTA CAA TTA CAA TG) and the specific primer 26.1 (5′-AAT CAT ACT AGT ACC GCC GGC CAG GT, for GPR) or 31.1 (5′-AAT CAT ACT AGT ACC GCC CAA GTA CTC CCA C, for R6A). After a *Bpm*I/*Spe*I digest, the dsDNA was co-ligated with synthesized, complementary linker oligos (5′-TCG AGC TCT GGA GGC ATC GAG GGT CGC AT and 5′-GCG ACC CTC GAT GCC TCC AGA GC) into pDW363A (Supporting Information) at the *Xho*I/*Spe*I sites to produce pDW363B-GPR and -R6A. These constructs encode the N-terminal biotinylation tag followed by a Factor Xa protease cut site, the inserted peptide, and a C-terminal MBP. L19 GPR was produced by site-directed mutagenesis (QuikChange, Stratagene) of pDW363B-GPR. Expression and cell lysate preparation of MBP (using pDW363A), L19 GPR-MBP, and R6A-MBP were performed as described above. The cleared lysates were purified on Streptavidin Sepharose (High Performance, Amersham) and washed thoroughly with pDW buffer (50 mM HEPES-KOH at pH 7.5, 200 mM NaCl, 1 mM EDTA, and 0.1% Triton X-100). After washing once with Xa buffer (50 mM HEPES-KOH at pH 7.5, 150 mM NaCl, and 1 mM $CaCl_2$), the protein was incubated on-column overnight with Factor Xa (20 units, Amersham) in Xa buffer at room temperature. Proteins were eluted with additional pDW buffer and the Factor Xa was removed with *p*-aminobenzamidine agarose

(Sigma). Purified proteins were desalted and concentrated in a Centriprep YM-30 into 1× PBS. A 50-mL culture yielded ~16 mg of >98% pure protein (~320 mg/L culture).

Binding Analysis by Surface Plasmon Resonance (SPR). Kinetic measurements were made at 25 °C on a Biacore 2000 instrument (Biacore, Inc., Piscataway, NJ) equipped with research-grade SA (streptavidin) sensor chips. Nb-$G_{i\alpha1}$ was immobilized to a surface density of ~1000 response units (RU). Modified HBS-EP [10 mM HEPES at pH 7.4, 150 mM NaCl, 3 mM EDTA, 0.005% polysorbate 20 (Tween 20), 8 mM $MgCl_2$, 30 μM GDP, and 0.05% (w/v) BSA] was used as the running buffer for all experiments. To collect kinetics data, a concentration series (25, 50, 2× 100, 200, 400, and 800 nM) for each peptide was injected for 2 min at a flow rate of 100 μL/min. Sample injections were interspersed with a number of buffer blank injections for double referencing with a negative control surface without $G_{i\alpha1}$ used to monitor background binding (*31*). Dissociation was allowed to continue for ~6 min between injections, which allowed the signal to return to baseline, alleviating the need for injecting a regeneration solution. Raw data were processed with Scrubber and globally fit with CLAMP using a 1:1 bimolecular interaction model (*32*). K_D values were calculated (k_d/k_a) from the rates determined by CLAMP. For weaker affinity peptides, higher concentrations were used and the K_D values were determined from equilibrium binding responses using Scrubber. Results from repeated experiments produced similar results, with K_D values within 50% of those shown.

For the analysis of G protein binding states, L19 GPR- and R6A-MBP were immobilized by standard amine-coupling to separate flow cells of an NHS/EDC-activated CM5 sensor chip (Biacore) to a surface density of ~200 RU. Activated flow cells were subsequently blocked with ethanolamine. $G_{i\alpha1}$ (1 μM final concentration) was incubated in HBS-EP+M (10 mM HEPES at pH 7.4, 150 mM NaCl, 3 mM EDTA, 0.005% polysorbate 20, and 8 mM $MgCl_2$) supplemented with 25 μM GDP, 25 μM GDP with 25 μM $AlCl_3$ and 10 mM NaF, or 25 μM GTPγS for ~1 h at 30 °C. G protein solutions were then injected for 3 min at 35 μL/min across all flow cells and allowed to dissociate for 3 min between injections. BIAevaluation software version 3.2 (Biacore) was used to background subtract all traces with data from a negative control flow cell containing immobilized MBP.

Aluminum Fluoride Activation. Fluorescence measurements were made on a spectrofluorophotometer (RF-5301PC, Shimadzu Scientific Instruments, Columbia, MD) with excitation and emission wavelengths set at 292 and 333 nm, respectively (slit widths at 3 and 5 nm, respectively). $G_{i\alpha1}$ (200 nM) was preincubated with and without 400 nM peptide in 2.5 mL of buffer A3 (buffer A supplemented with 100 μg/mL BSA, 1 mM β-mercaptoethanol, and 5 μM GDP) at 25 °C for 15 min prior to starting the experiment. The temperature throughout the experiment was maintained at 25 °C using a circulating bath (RTE-101, Thermo NESLAB, Portsmouth, NH). Fluorescence was measured for 850 s with a data collection rate of 3 Hz. G proteins were activated by quickly adding 0.5 M NaF (2 mM final concentration) and 10 mM $AlCl_3$ (30 μM final concentration) at 150 and 200 s, respectively. Samples without $G_{i\alpha1}$ were used for baseline subtraction. Traces were smoothed by 5-point adjacent averaging using Origin 6.0 Professional (OriginLab Corp., Northampton, MA).

GTPγS Binding. Solutions of $G_{i\alpha1}$ with varying concentrations of peptide were incubated in buffer B (20 mM HEPES-KOH at pH 7.5, 200 mM NaCl, 1 mM EDTA, 5 mM $MgCl_2$, 1 mM DTT, 0.005% Tween 20, and 100 μg/mL BSA) for ~20 min at room temperature. All measurements were made in black bottom 96-well plates (Nalge Nunc International, Rochester, NY). Reactions were initiated by diluting the $G_{i\alpha1}$ (100 nM final concentration) samples into BODIPY FL GTPγS (0.8 μM final concentration, Molecular Probes, Eugene, OR) in buffer B using a multichannel pipet, mixing by pipet, and scanning immediately in kinetics mode on a fluorescence plate reader (Flexstation, Molecular Devices, Sunnyvale, CA) for 6 h (45 s between reads, 15 reads/well) at ambient temperature (~25 °C). Excitation and emission wavelengths were set at 485 and 530 nm, respectively, and a 515 nm cutoff filter was used. PMT detection was set at high sensitivity. Data analysis and background subtraction of reactions without the protein were performed with Softmax Pro 4.3.1 (Molecular Devices). Fluorescence curves were fit to single [$A(1 - e^{-kt})$] or double [$A(1 - e^{-kt}) + A_2(1 - e^{-k_2 t})$] exponential equations using Origin 6.0.

Immunoprecipitation. The interaction between $G_{i\alpha1}$ and $G_{\beta1\gamma2}$ subunits in the presence and absence of GPR-derived peptides was assayed using purified G protein subunits. Nb-$G_{i\alpha1}$ (40 ng) in 0.5 mL of IP buffer [25 mM HEPES-KOH at pH 7.5, 150 mM NaCl, 5 mM EDTA, 10 mM $MgCl_2$, 1 mM DTT, 0.05% Tween 20, 0.1% (w/v) BSA, and 30 μM GDP or GTPγS] was supplemented with varying concentrations of the indicated peptide (0, 25, 250, and 2500 nM) and incubated at room temperature for 30 min. After addition of $G_{\beta1\gamma2}$ (50 ng, Calbiochem-Novabiochem Corp., La Jolla, CA) and incubation at 4 °C for several hours, NeutrAvidin-agarose (10 μL) was added and the samples were rotated overnight. The agarose was washed with 3× 0.5 mL of IP buffer in a 0.45-μm spin filter and resuspended in 2× SDS-loading buffer. Resuspended samples were incubated at 90 °C for 5 min prior to SDS−PAGE analysis. Proteins were electrotransferred to PVDF membranes (Amersham) and analyzed by Western blot using anti-G_β BN1 (1:5000) and anti-rabbit peroxidase (1:8000, Roche) as the primary and secondary antibodies, respectively, and an ECL Plus kit for detection (Amersham).

RESULTS

$G_{i\alpha1}$ as a Target for Peptide Selection. Specifically biotinylated $G_{i\alpha1}$ subunits were expressed and purified to provide homogeneously presented targets for the peptide selection experiments. The recombinant proteins Nb- and Cb-$G_{i\alpha1}$ contain a single N- or C-terminal biotin tag, respectively, and were produced by different techniques, as described in the Experimental Procedures (Figure 1B). Both Nb- and Cb-$G_{i\alpha1}$ were protected from trypsin digest after loading with GTPγS (data not shown), demonstrating that the proteins were active for nucleotide exchange (*33*, *34*). The biotinylated $G_{i\alpha1}$ subunits were also tested for their ability to pull down the GPR consensus peptide, a sequence derived from the 4 GPR motif repeats of AGS3 (Figure 1C) (*20*). Radioactively labeled GPR RNA-peptide fusions were purified and assayed for binding against $G_{i\alpha1}$, immobilized

on streptavidin agarose. Binding of the fusions was specific for Nb- and Cb-$G_{i\alpha1}$ (80 and 30% binding, respectively) over the streptavidin-agarose matrix (0% binding). The binding of the GPR motif as an RNA-peptide fusion demonstrated the feasibility of performing further in vitro selection experiments using mRNA display of GPR-derived peptides. Because subsequent GPR-derived libraries would encode M19L and V24S mutations to facilitate library construction (L19 and S24 are "allowed" residues that are included in a number of the GPR motif repeats within AGS3), these mutants were also assayed for binding.[2] RNA-peptide fusions of M19L or V24S GPR demonstrated negligible differences in binding to immobilized $G_{i\alpha1}$ compared to the fusions of the "wild-type" GPR consensus sequence (data not shown).

X23 Control Library. A control selection experiment using the GPR X23 library (Figure 1C) was performed against Nb- and Cb-$G_{i\alpha1}$ to evaluate the proteins as selection targets. R23 is a key amino acid in the GPR motif, because mutations to R23 greatly reduce or eliminate binding to $G_{i\alpha1}$ (*20*, *35*, *36*). Reverse-transcribed RNA-peptide fusions of the X23 library were allowed to bind to immobilized $G_{i\alpha1}$, nonbinding fusions were removed with buffer washes, and viable peptide sequences were determined by PCR amplification of recovered cDNA and DNA sequencing of individual clones (Figure 1A). After 1 round of selection, 70% (4 of 6 sequences) and 80% (5 of 6 sequences) Arg at position 23 were recovered against the Nb- and Cb-$G_{i\alpha1}$ matrixes, respectively, compared with 0% (0 of 6 sequences) for the original X23 pool.

In Vitro Selection with C-GPR Extension Library. Because R23, which marks the C-terminal residue of the conserved GPR motif, was determined to be crucial for G protein interaction, a C-terminal "extension" library was synthesized to establish whether amino acids just outside of the conserved region affect binding. The C-GPR X6 library (Figure 1C) also included an N-terminal truncation to reduce the binding affinity of the initial pool, allowing for higher enrichment of functional peptides. The initial pool of RNA-peptide fusions contained at least 10^{12} sequences, well encompassing the possible number of unique sequences in a random 6-mer library ($20^6 = 6.4 \times 10^7$ unique sequences). A total of 6 rounds of selection were performed on a mixture of immobilized Nb- and Cb-$G_{i\alpha1}$ to reduce the effects of bias or steric hindrance with either terminus immobilized (Figure 2A). Detergent, bovine serum albumin (BSA), and salt were included in selection buffers to minimize recovery of nonspecific binding peptides. DNA sequencing of the 6th round pool revealed a dominant peptide sequence, R6A (Figure 2B).

To recover other rare sequences that were active for binding, mRNA encoding R6A was removed by subtractive hybridization. After an additional 2 rounds of selection, each preceded by a subtractive hybridization step (Figure 2A), a variety of sequences with high similarity to R6A were discovered, revealing the conserved residues of the selected peptides (Figure 2B). Surprisingly, mutations were discovered in the constant region of R6A for all selected peptides, including the crucial R23. Despite the subtractive hybridization steps, sequences of R6A were still recovered after the 8th round, demonstrating the high selectivity for this peptide sequence.

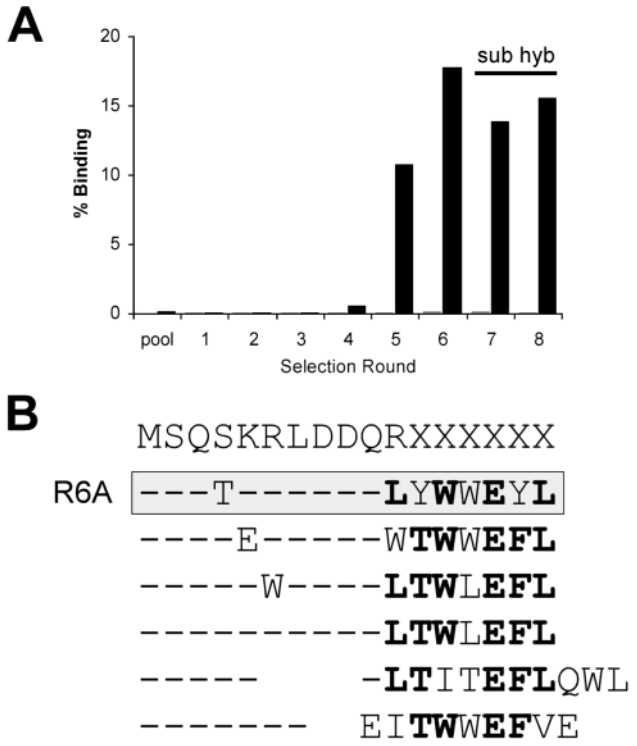

FIGURE 2: (A) Selection of the C-GPR X6 extension library against $G_{i\alpha1}$. ^{35}S-methionine-labeled RNA-peptide fusions from each round of selection and the original pool were assayed for binding to immobilized $G_{i\alpha1}$ (black) or to the matrix alone (gray). Subtractive hybridization (sub hyb) was performed prior to the 7th and 8th rounds of selection to remove the dominant sequence, R6A. (B) Sequences of selected peptides. A dash indicates the same residue as the wild type (C-GPR X6 library). Sequences with internal deletions (spaces) have been aligned by their conserved residues (bold). R6A (boxed) was the dominant peptide from the 6th round of selection, which also reemerged after round 8 despite the subtractive hybridization step. The C-terminal constant region, which was frame-shifted in sequences with deletions, is not shown.

A separate binding assay with RNA-peptide fusions from the 6th round of selection demonstrated the same preference for Nb-$G_{i\alpha1}$ (40% pull-down) over Cb-$G_{i\alpha1}$ (4%) as with the GPR consensus fusions, further indicating that GPR and GPR-derived peptides favor $G_{i\alpha1}$ immobilized via the N terminus.

GPR-Derived Peptides Favor the GDP-Bound State of $G_{i\alpha1}$. To assay the nucleotide dependence of the GPR-derived peptides for $G_{i\alpha1}$, binding interactions were observed in real time using SPR. N-terminal L19 GPR or R6A peptide fusions with maltose-binding protein (MBP) were immobilized by random amine coupling to biosensor surfaces. $G_{i\alpha1}$ subunits, preincubated with either GDP (to maintain the inactive, GDP-bound state), GDP with AlF_4^- (to mimic the transition state of GTP hydrolysis), or GTPγS (a nonhydrolyzable GTP analogue to mimic the active, GTP-bound state), were injected across these surfaces (Figure 3A). Both the L19 GPR- and R6A-MBP proteins favored the GDP-bound state of $G_{i\alpha1}$, although L19 GPR demonstrated detectable binding for the other states as well. No binding was detected in a control cell containing immobilized MBP.

Several GPR-derived peptides were also synthesized and purified for kinetic analysis by SPR. Nb-$G_{i\alpha1}$ was im-

[2] Numbering of residues is based on the GPR consensus peptide (*20*), starting with Thr1 and ending with Gly28 (Figure 1C).

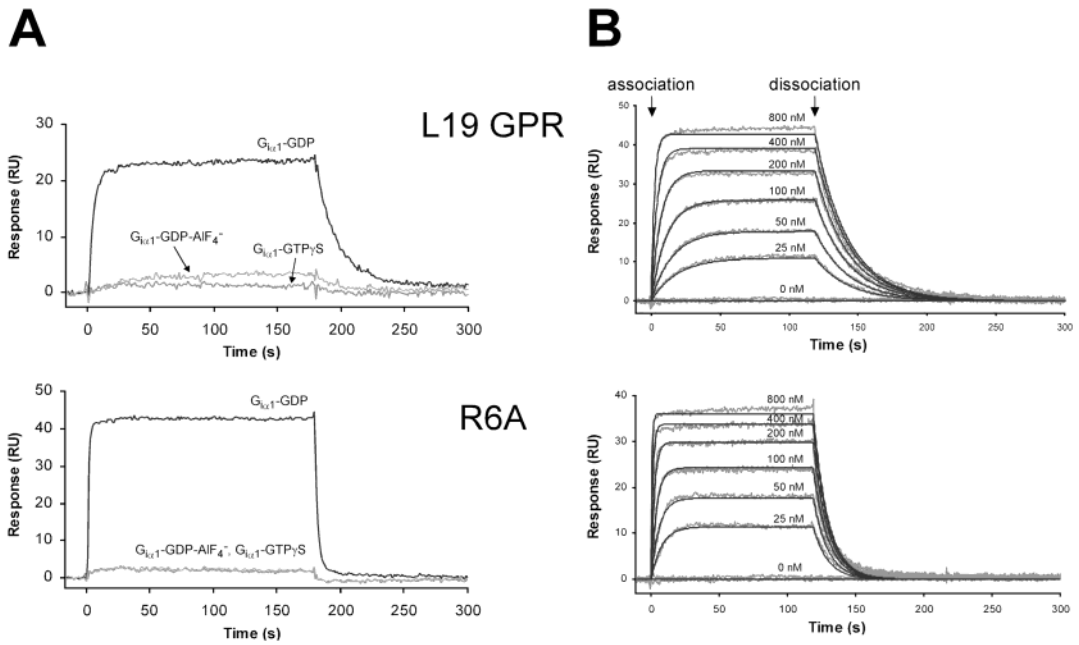

FIGURE 3: Binding interactions studied by SPR. (A) L19 GPR and R6A specifically recognize the GDP-bound state of $G_{i\alpha1}$. L19 GPR- and R6A-MBP fusion proteins (top and bottom, respectively) were immobilized by amine coupling in separate flow cells to a surface density of ~200 RU. State specificity of the GPR-derived peptides was determined by injection (105 μL at 0 s, with a 35 μL/min flow rate) of preformed $G_{i\alpha1}$-GDP, $G_{i\alpha1}$-GDP-AlF_4^-, or $G_{i\alpha1}$-GTPγS (at 1 μM $G_{i\alpha1}$). (B) Kinetics of peptide interaction with $G_{i\alpha1}$-GDP. A peptide concentration series of L19 GPR (top) and R6A (bottom) was injected (200 μL at 0 s, with a 100 μL/min flow rate) across ~1000 RU of immobilized Nb-$G_{i\alpha1}$, maintained in the GDP-bound state. The global kinetic fits (black) are overlaid on the original sensorgrams (gray). The derived kinetic parameters are shown in Table 1. Sensorgrams have been double-referenced from response curves generated by an appropriate negative control flow cell and averaged buffer blank injections.

Table 1: Kinetic Parameters for Binding of Various Peptides with $G_{i\alpha1}$-GDP, Determined by SPR[a]

	peptide	k_a [M^{-1} s^{-1} ($\times$ 10^5)]	k_d [s^{-1} ($\times$ 10^{-2})]	K_D (nM)	χ^2
L19 GPR	TMGEEDFFDLLAKSQSKRLDDQRVDLAGYK	5.03 (1)	4.139 (7)	82	0.61
L19 GPR R23L	TMGEEDFFDLLAKSQSKRLDDQLVDLAGYK			14 000	
R6A	MSQTKRLDDQLYWWEYL	15.51 (6)	9.28 (3)	60	0.76
R6A-1	DQLYWWEYL			200	
R6A-R	DQRYWWEYL			15 000	
C-GPR	MSQSKRLDDQRVDLAGYK			NB	

[a] K_D values were calculated (k_d/k_a) from kinetic parameters when available. Other K_D values were obtained by fitting steady-state binding responses. The number in parentheses represents the error in the last digit from fittings. The C-GPR control peptide was nonbinding (NB) at concentrations up to 20 μM.

mobilized on streptavidin-coated sensor chips and the binding of various concentrations of injected peptide was monitored (Figure 3B). The GDP-bound state of $G_{i\alpha1}$ was maintained by supplementing the running buffer with GDP. The running buffer also contained BSA, which was crucial for minimizing nonspecific binding and obtaining high quality data. Kinetic parameters were derived from globally fitting the data with a 1:1 interaction model, resulting in dissociation constants (K_D) of 82 nM for L19 GPR and 60 nM for R6A (Table 1) (*31*).

To determine a minimal binding peptide sequence, N-terminal truncations of R6A were also assayed by SPR. The shortest peptide tested, R6A-1, bound to $G_{i\alpha1}$ with a K_D of ~200 nM. Shorter peptides were not synthesized because of the hydrophobicity of the C terminus of R6A. While the control C-GPR peptide did not bind to Nb-$G_{i\alpha1}$ at concentrations up to 20 μM, the mutant peptides R6A-R and L19 GPR R23L both demonstrated >100-fold weaker affinities (determined by fitting steady-state binding measurements) compared to their parent sequences (Table 1). The full-length R6A library construct (with the C-terminal QLRNSCA tag) exhibited a similar affinity for $G_{i\alpha1}$ as R6A, indicating that the constant region did not bias the selection (data not shown). Using Cb-$G_{i\alpha1}$ as the immobilized ligand resulted in significantly lower affinities, confirming the preference for $G_{i\alpha1}$ immobilized via the N terminus (data not shown). The K_D values determined for L19 GPR and R6A were verified by fluorescence titration experiments using C-terminal fluorescein-conjugated peptides (data not shown).

GPR and R6A Act as GDIs. GPR-derived peptides stabilize the GDP-bound state of $G_{i\alpha1}$ and inhibit the activation of $G_{i\alpha1}$ with aluminum fluoride (*37*). Binding of AlF_4^- causes an increase in intrinsic tryptophan fluorescence, which can be measured in real time by spectrofluorometry. While preincubation of $G_{i\alpha1}$ with the C-GPR control peptide had little effect, both the L19 GPR and R6A peptides significantly reduced aluminum fluoride activation, suggesting that R6A retains GDI activity (Figure 4A).

GDI activity of the peptides was also assayed by directly observing nucleotide exchange in $G_{i\alpha1}$. BODIPY FL GTPγS is a fluorescent, nonhydrolyzable analogue of GTP that self-quenches in solution. Upon binding to a G_α subunit, however, this analogue exhibits an increase in fluorescence, allowing real-time and high-throughput monitoring of GTP loading

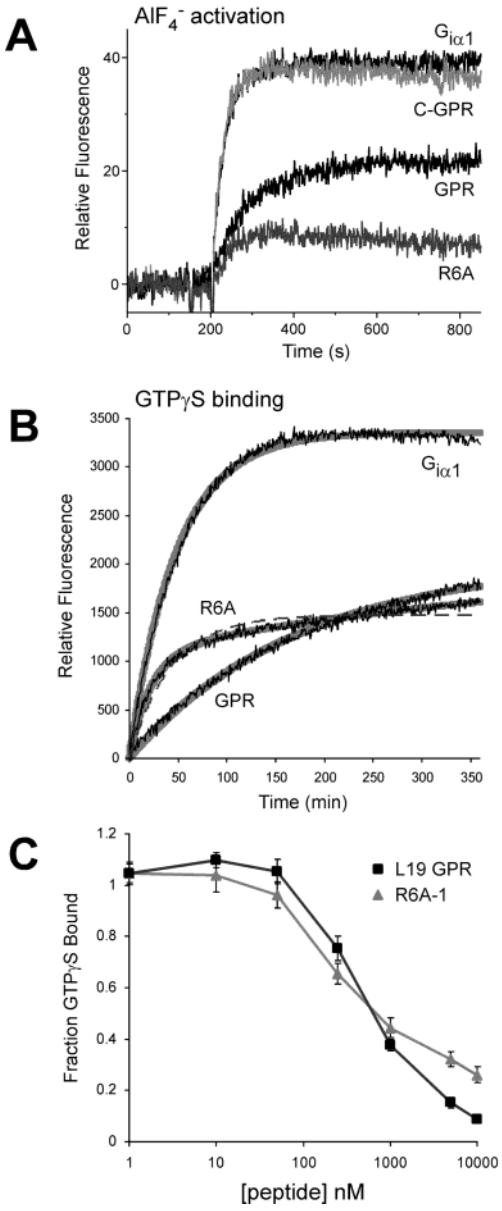

FIGURE 4: GDI activity. (A) GPR-derived peptides stabilize the GDP-bound state of $G_{i\alpha1}$. Tryptophan fluorescence, which is enhanced upon activation by AlF_4^-, was measured on $G_{i\alpha1}$ (200 nM) preincubated with and without 400 nM peptide (L19 GPR, R6A, or C-GPR negative control). NaF and $AlCl_3$ were added at 150 and 200 s, respectively. The average fluorescence of the first 150 s was set to zero, and all response curves were background-subtracted with a buffer or peptide blank sample. (B) GPR-derived peptides inhibit binding of a fluorescent GTPγS analogue. Binding of BODIPY FL GTPγS to $G_{i\alpha1}$ causes an enhancement of fluorescence, which is measured in real time. $G_{i\alpha1}$ (100 nM final concentration) is preincubated with and without the indicated peptide (1 μM final concentration) prior to dilution into a buffer containing BODIPY FL GTPγS (0.8 μM final concentration). After mixing, the measurements are quickly initiated in a fluorescence plate reader, allowing up to 96 samples to be assayed simultaneously. While the GPR and $G_{i\alpha1}$ without peptide inhibitor curves can be fit with single exponentials (gray), the R6A fluorescence curve appears biphasic, requiring a double exponential (gray) to fit appropriately (dotted line shows the single exponential fit). Fluorescence curves have been background-subtracted with data generated from samples lacking $G_{i\alpha1}$. (C) Peptide concentration dependence of BODIPY FL GTPγS binding. Data for L19 GPR (■) and R6A-1 (▲) are expressed as a fraction of fluorescence (± standard deviation) observed in the absence of peptide inhibitor at 180 min.

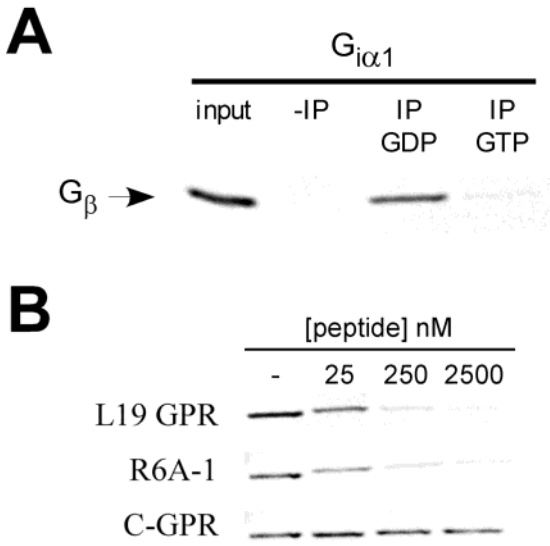

FIGURE 5: (A) $G_{\beta1\gamma2}$ subunits coprecipitate with $G_{i\alpha1}$-GDP. Nb-$G_{i\alpha1}$ reconstituted in vitro with $G_{\beta1\gamma2}$ subunits was precipitated with streptavidin agarose. The equivalent of ~33 ng of $G_{\beta1\gamma2}$ was run in each lane, and membrane transfers were probed with a G_β antiserum. Preincubation of the G proteins with GTPγS prevented association and coprecipitation of G_β subunits. The −IP lane is a pull-down without Nb-$G_{i\alpha1}$. Approximately 60% of input $G_{\beta1}$ was precipitated in a 1:1 molar mix of Nb-$G_{i\alpha1}$ and $G_{\beta1\gamma2}$. (B) L19 GPR and R6A-1 peptides compete with $G_{\beta1\gamma2}$ for binding to $G_{i\alpha1}$. Reconstituted $G_{i\alpha1\beta1\gamma2}$ was preincubated with increasing concentrations of the indicated peptide prior to precipitation and probing as in (A). The C-GPR control peptide did not compete for binding. Full-length R6A acted comparably to the minimal peptide (data not shown).

(*38*). The L19 GPR and R6A-1 peptides (1 μM), each preincubated with $G_{i\alpha1}$, reduced the initial rate of BODIPY FL GTPγS binding to ~20 and ~70%, respectively, of the initial rate for $G_{i\alpha1}$ without peptide. After 180 min, however, both peptides demonstrated similar equilibrium inhibition activities, reducing the fluorescence to ~40% of the fluorescence of BODIPY FL GTPγS-bound $G_{i\alpha1}$ without peptide inhibitor (Figure 4B). This disparity is caused by the biphasic kinetics of GTP binding for $G_{i\alpha1}$ incubated with R6A-derived peptides.

The L19 GPR and $G_{i\alpha1}$ without peptide fluorescence curves fit well to single exponentials, and the GDI activity with L19 GPR was fairly well-modeled by the simple scheme: G_α-GDP-GPR ↔ G_α-GDP ↔ G_α ↔ G_α-GTP (data not shown). The curves generated with higher concentrations (>50 nM) of R6A-derived peptides, however, require a more complex inhibition model and were better described by double exponential equations, which reveal a fast, "burst" phase and a ~10-fold slower second phase (Figure 4B). Both phases contribute significantly to the fluorescence amplitude (the slow phase represents 20−70% of the total amplitude depending on the inhibitor concentration). Appropriate blanks (with BODIPY FL GTPγS and peptide inhibitor but without $G_{i\alpha1}$) and controls with the R6A-R mutant peptide suggested that the effect was specific and not the result of background fluorescence or nonspecific binding. The rate constants of the slow phase did not appear to correlate with peptide concentration, suggesting a parallel reaction pathway. Inhibition with R6A was similar to that of the minimal peptide, R6A-1 (see the Supporting Information to view the concentration series for all peptides).

IC_{50} values could be determined from the overall fluorescence at 180 min of BODIPY FL GTPγS-bound $G_{i\alpha1}$ with and without various concentrations of the peptide inhibitor. L19 GPR and R6A-1 demonstrated comparable submicromolar IC_{50} values ($\sim$0.5 μM, Figure 4C), while the mutant peptides, L19 GPR R23L and R6A-R, demonstrated IC_{50} values consistent with their lower binding affinities (IC_{50} > 10 μM, data not shown). IC_{50} values determined by the peptide concentration dependence of the initial rate of BODIPY FL GTPγS binding were severely skewed for R6A-derived peptides because of the initial fast phase of binding (data not shown). Incubation with the C-GPR control peptide at concentrations up to 10 μM had no effect on either the initial rate or the steady-state fluorescence.

$G_{\beta\gamma}$ Competition. Although GPR-derived peptides stabilize the inactive, GDP-bound state of $G_{i\alpha}$ subunits, previous studies demonstrated that the GPR motif competes with $G_{\beta\gamma}$ for binding to $G_{i\alpha}$-GDP, promoting subunit dissociation and $G_{\beta\gamma}$-specific signaling in the absence of nucleotide exchange (*14*). To examine this for the selected peptides, reconstituted $G_{i\alpha1\beta1\gamma2}$ was used in coprecipitation experiments. Control experiments first established that $G_{\beta1}$ subunits coprecipitated with $G_{i\alpha1}$ in the GDP state but not in the GTPγS-bound state (Figure 5A). To assay $G_{\beta\gamma}$ competition, increasing concentrations of peptide were incubated with the G protein prior to precipitation. Both the L19 GPR and R6A-1 peptides competed with $G_{\beta\gamma}$ for binding to $G_{i\alpha1}$ (Figure 5B). Results for the full-length R6A peptide were similar (data not shown).

DISCUSSION

The GPR consensus peptide is the shortest, most potent peptide GDI known for the G_i family of G proteins (*20*). To demonstrate the feasibility of using in vitro selection to develop peptides with varying activities and specificities for various G protein α subunits, the GPR motif was used as a starting point for mRNA display selection experiments, which requires immobilization of a target protein (*12*). Because G_α subunits putatively contain many regulatory/effector sites, random immobilization schemes (e.g., random amine coupling or biotinylation of surface cysteine residues) that might restrict binding to favorable, "hot-spots" for protein interaction (*39*) were avoided. Instead, specific biotinylation of the N or C terminus of $G_{i\alpha1}$ was accomplished using two different methods: in vivo biotinylation with *E. coli* biotin holoenzyme synthetase (*23*) and chemical ligation (*25*, *26*). Both of these methods provided ample protein yields for the selection and subsequent assays. The *E. coli* in vivo biotinylation expression system was especially favorable because protein minipreps (5 mL) yielded sufficient material for hundreds of kinetics measurements by SPR.

In vitro selection with an extension library, where the conserved region of the GPR motif was extended by six random residues on the C terminus, revealed a dominant peptide, R6A, as well as other highly similar sequences. Only the C-terminal half of the GPR motif was used in the library to allow for higher enrichment of viable peptides and to serve as an "anchor" for the selection, producing peptides that bound near the nucleotide-binding pocket. Surprisingly, selected peptides all contained mutations in the designed, conserved region, including the crucial R23. R6A and the L19 GPR peptide demonstrated comparable binding affinities for $G_{i\alpha1}$ based on SPR and fluorescence titration experiments although the association and dissociation rates were several fold faster for R6A.

N-terminal truncations of R6A bound nearly as well as the full-length peptide. The shortest peptide tested, R6A-1, is a 9-residue sequence that also retains both high-affinity binding and GDI activity for $G_{i\alpha1}$. Because R6A-1 preserves only two of the original residues from the C terminus of the GPR motif, this raises the possibility that the R23L mutation eliminated any "anchoring" effect that the constant region had for the nucleotide-binding pocket of $G_{i\alpha1}$ and allowed the library to localize to other regions. Several assays suggested that this was not the case. Both R6A and L19 GPR peptides favored binding to $G_{i\alpha1}$ immobilized by the N terminus rather than by the C terminus. This may result from steric hindrance because Cb-$G_{i\alpha1}$ was produced without the long peptide linker region that Nb-$G_{i\alpha1}$ includes. The peptides also competed with each other for binding to $G_{i\alpha1}$ based on SPR as well as radioactively labeled pull-down experiments (data not shown). These results suggest that R6A and the GPR motif bind to the same or overlapping sites on $G_{i\alpha1}$, though this is not conclusive because binding to other regions (e.g., the flexible switch regions) could cause allosteric competition. The GDI activity of $G_{\beta1\gamma2}$, for example, stems from a rearrangement of switch regions I and II on $G_{i\alpha1}$, inducing new contacts with and tighter binding of GDP (*40*).

More surprising were observations that the minimal peptide, R6A-1, as well as its parent sequence, retained the ability to compete with $G_{\beta\gamma}$ subunits for binding to $G_{i\alpha1}$. The $G_{i\alpha1}$-GPR (GoLoco) crystal structure revealed direct contacts between the C terminus of the GPR motif with the GDP-binding pocket and the N terminus with switch II of $G_{i\alpha1}$, which is perturbed such that $G_{\beta\gamma}$ can no longer bind (*35*). R6A-1 is not long enough, however, to fully span the same regions, implying that binding, GDI, and/or $G_{\beta\gamma}$ competition activities are produced by long-range effects. It is difficult to predict how the 9-residue R6A-1 could affect the switch II region as extensively as the GPR consensus peptide, though perturbation of switch I from the nucleotide-binding site could lead to a restructuring of the switch regions and subsequent loss of $G_{\beta\gamma}$ binding.

Although the selected peptides are similar to the GPR consensus sequence in binding affinity and GDI activity for $G_{i\alpha1}$, aberrant inhibition kinetics were observed in the nucleotide exchange experiments using the BODIPY-labeled GTP analogue. The inhibition by GPR was easily described by a direct competition model; however, we were unable to determine a kinetics model describing the biphasic GTP-binding curves from R6A-inhibited experiments. The double exponential fits suggest an alternate reaction pathway with a different reaction rate. Proposed models were unable to correlate the fast, initial phase of GTP-binding with the binding kinetics of the R6A peptide for $G_{i\alpha1}$-GDP determined by the SPR experiments. These peptide signal modulators may be useful in systems where it is desirable to attenuate the overall G protein activation, without significantly perturbing the initial kinetics.

Several studies have demonstrated the importance of neighboring residues outside of the conserved region of the GPR motif. Replacement of the nonconserved residues

C-terminal to R23 of the GPR consensus sequence with a short peptide linker greatly reduces binding affinity for $G_{i\alpha1}$ (data not shown), demonstrating that flanking residues can strongly modulate the binding affinity. With the GPR (GoLoco) motif of RGS14, nonconserved C-terminal residues convey specificity for $G_{i\alpha}$ over $G_{o\alpha}$ subunits, winding through the helical domain and contacting $G_{i\alpha}$-specific residues (*35*). More recently, a comprehensive study of the four GPR motif repeats of activator of G protein signaling 3 (AGS3) confirmed that residues outside of the conserved GPR motifs strongly potentiate binding and GDI activity for $G_{i\alpha1}$ (*41*). Studies with R6A and other peptides isolated from the selection may reveal additional specificities and activities for other G_α subunits.

The arginine finger has been a common theme in guanine nucleotide-binding proteins and GTPase activity (*35*, *42*−*45*). In $G_{i\alpha1}$, for example, R178 within switch I stabilizes the γ-phosphate leaving group and is crucial for GTPase activity (*43*). The $G_{i\alpha1}$-GPR structure revealed extensive contacts with the nucleotide-binding pocket of $G_{i\alpha1}$ and the conserved tripeptide, Asp-Gln-Arg (Arg equivalent to R23 on the GPR consensus peptide), from the GPR motif. The Asp and Gln residues are positioned away from the GDP-binding site allowing the Arg residue to insert into the pocket and form hydrogen bonds with the α and β phosphates and their bridging oxygen (*35*). Mutation of Arg on the GPR motif has been shown to substantially diminish or eliminate GDI activity and binding affinity for $G_{i\alpha}$ (*20*, *35*, *36*). From our SPR experiments, the R23L mutation on the GPR consensus peptide resulted in a ~170-fold lower binding affinity ($\Delta\Delta G^\circ = 3.0$ kcal/mol). It is unclear how the selected peptides bind and stabilize the GDP-bound state of $G_{i\alpha1}$ without an Arg residue and whether the remaining conserved residues form the same contacts as in the GPR motif. However, the Arg to Leu mutation isolated by selection is crucial for binding and activity, as demonstrated by studies on the R6A-R peptide ($\Delta\Delta G^\circ = 2.6$ kcal/mol between R6A-1 and R6A-R). Structural analysis of the $G_{i\alpha1}$-R6A complex will provide more insight into the mechanism of inhibition for the selected peptides.

We have demonstrated the use of mRNA display for the in vitro selection of peptides with high affinity for $G_{i\alpha1}$. By fine tuning the selection methodology, we may be able to further modulate peptide GDI or $G_{\beta\gamma}$ competition activity or adjust the kinetics of G protein activation. The minimal 9-mer peptide, R6A-1, can serve as a short scaffold for the selection of new peptide sequences with affinity and specificity for other G_α targets. The recent development of mRNA display libraries of peptide-drug conjugates may facilitate the selection of molecules consisting of GDP or GTP analogues covalently coupled to peptides optimized for G_α selectivity (*46*). Selections on G proteins in various nucleotide-bound states may produce other peptide regulators that act as GDIs, GEFs, or GAPs. Small peptide modulators of G protein signaling will be useful for probing G protein function as well as serve as starting points for G protein-specific drug design (*5*, *6*).

ACKNOWLEDGMENT

We thank Prof. Roger K. Sunahara (University of Michigan) for the G protein expression vector, Dr. David S. Waugh (National Cancer Institute at Frederick) for the in vivo biotinylation vector, Prof. Melvin I. Simon and Valeria Mancino for the polyclonal G_β antiserum and use of the Flexstation fluorescence plate reader, Prof. Pamela J. Bjorkman and Anthony M. Giannetti for time and technical assistance on their Biacore 2000 instrument, and Prof. Douglas C. Rees and Terry Takahashi for helpful discussions on the kinetics models. Prof. David G. Myszka (University of Utah) generously provided the analysis software, Scrubber and CLAMP. We greatly appreciate the preparative and technical expertise on protein purification provided by Dr. Shuwei Li (University of Texas Southwestern Medical Center) and Christopher T. Balmaseda. We are also grateful to Dr. Judy E. Kim for comments on the paper.

SUPPORTING INFORMATION AVAILABLE

Real-time fluorescence data of BODIPY FL GTPγS binding to $G_{i\alpha1}$ in the presence of various peptides (concentration series), construction of the pDW363A vector, and synthesis of the biotinyl-cysteine derivative. This material is available free of charge via the Internet at http://pubs.acs.org.

REFERENCES

1. Gilman, A. G. (1987) G proteins: Transducers of receptor-generated signals, *Annu. Rev. Biochem. 56*, 615−649.
2. Neves, S. R., Ram, P. T., and Iyengar, R. (2002) G protein pathways, *Science 296*, 1636−1639.
3. Higashijima, T., Ferguson, K. M., Sternweis, P. C., Smigel, M. D., and Gilman, A. G. (1987) Effects of Mg^{2+} and the $\beta\gamma$-subunit complex on the interactions of guanine nucleotides with G proteins, *J. Biol. Chem. 262*, 762−766.
4. Vetter, I. R., and Wittinghofer, A. (2001) The guanine nucleotide-binding switch in three dimensions, *Science 294*, 1299−1304.
5. Höller, C., Freissmuth, M., and Nanoff, C. (1999) G proteins as drug targets, *Cell. Mol. Life Sci. 55*, 257−270.
6. Nürnberg, B., Tögel, W., Krause, G., Storm, R., Breitweg-Lehmann, E., and Schunack, W. (1999) Non-peptide G-protein activators as promising tools in cell biology and potential drug leads, *Eur. J. Med. Chem. 34*, 5−30.
7. Dower, W. J., and Mattheakis, L. C. (2002) *In vitro* selection as a powerful tool for the applied evolution of proteins and peptides, *Curr. Opin. Chem. Biol. 6*, 390−398.
8. Lin, H., and Cornish, V. W. (2002) Screening and selection methods for large-scale analysis of protein function, *Angew. Chem., Int. Ed. 41*, 4402−4425.
9. Martin, E. L., Rens-Domiano, S., Schatz, P. J., and Hamm, H. E. (1996) Potent peptide analogues of a G protein receptor-binding region obtained with a combinatorial library, *J. Biol. Chem. 271*, 361−366.
10. Scott, J. K., Huang, S. F., Gangadhar, B. P., Samoriski, G. M., Clapp, P., Gross, R. A., Taussig, R., and Smrcka, A. V. (2001) Evidence that a protein−protein interaction 'hot spot' on heterotrimeric G protein $\beta\gamma$ subunits is used for recognition of a subclass of effectors, *EMBO J. 20*, 767−776.
11. Ghosh, M., Peterson, Y. K., Lanier, S. M., and Smrcka, A. V. (2003) Receptor- and nucleotide exchange-independent mechanisms for promoting G protein subunit dissociation, *J. Biol. Chem. 278*, 34747−34750.
12. Roberts, R. W., and Szostak, J. W. (1997) RNA-peptide fusions for the *in vitro* selection of peptides and proteins, *Proc. Natl. Acad. Sci. U.S.A. 94*, 12297−12302.
13. Takahashi, T. T., Austin, R. J., and Roberts, R. W. (2003) mRNA display: Ligand discovery, interaction analysis, and beyond, *Trends Biochem. Sci. 28*, 159−165.
14. Bernard, M. L., Peterson, Y. K., Chung, P., Jourdan, J., and Lanier, S. M. (2001) Selective interaction of AGS3 with G-proteins and the influence of AGS3 on the activation state of G-proteins, *J. Biol. Chem. 276*, 1585−1593.

15. Natochin, M., Gasimov, K. G., and Artemyev, N. O. (2001) Inhibition of GDP/GTP exchange on Gα subunits by proteins containing G-protein regulatory motifs, *Biochemistry 40*, 5322−5328.
16. De Vries, L., Fischer, T., Tronchère, H., Brothers, G. M., Strockbine, B., Siderovski, D. P., and Farquhar, M. G. (2000) Activator of G protein signaling 3 is a guanine dissociation inhibitor for $G\alpha_i$ subunits, *Proc. Natl. Acad. Sci. U.S.A. 97*, 14364−14369.
17. Kimple, R. J., De Vries, L., Tronchère, H., Behe, C. I., Morris, R. A., Farquhar, M. G., and Siderovski, D. P. (2001) RGS12 and RGS14 GoLoco motifs are $G\alpha_i$ interaction sites with guanine nucleotide dissociation inhibitor activity, *J. Biol. Chem. 276*, 29275−29281.
18. Natochin, M., Lester, B., Peterson, Y. K., Bernard, M. L., Lanier, S. M., and Artemyev, N. O. (2000) AGS3 inhibits GDP dissociation from Gα subunits of the G_i family and rhodopsin-dependent activation of transducin, *J. Biol. Chem. 275*, 40981−40985.
19. Kimple, R. J., Willard, F. S., and Siderovski, D. P. (2002) The GoLoco motif: Heralding a new tango between G protein signaling and cell division, *Mol. Interventions 2*, 88−100.
20. Peterson, Y. K., Bernard, M. L., Ma, H., Hazard, S., Graber, S. G., and Lanier, S. M. (2000) Stabilization of the GDP-bound conformation of Giα by a peptide derived from the G-protein regulatory motif of AGS3, *J. Biol. Chem. 275*, 33193−33196.
21. Takesono, A., Cismowski, M. J., Ribas, C., Bernard, M., Chung, P., Hazard, S., Duzic, E., and Lanier, S. M. (1999) Receptor-independent activators of heterotrimeric G-protein signaling pathways, *J. Biol. Chem. 274*, 33202−33205.
22. Lee, E., Linder, M. E., and Gilman, A. G. (1994) Expression of G-protein α subunits in *Escherichia coli*, *Methods Enzymol. 237*, 146−164.
23. Tsao, K.-L., DeBarbieri, B., Michel, H., and Waugh, D. S. (1996) A versatile plasmid expression vector for the production of biotinylated proteins by site-specific, enzymatic modification in *Escherichia coli*, *Gene 169*, 59−64.
24. Chong, S. R., Mersha, F. B., Comb, D. G., Scott, M. E., Landry, D., Vence, L. M., Perler, F. B., Benner, J., Kucera, R. B., Hirvonen, C. A., Pelletier, J. J., Paulus, H., and Xu, M.-Q. (1997) Single-column purification of free recombinant proteins using a self-cleavable affinity tag derived from a protein splicing element, *Gene 192*, 271−281.
25. Lesaicherre, M.-L., Lue, R. Y. P., Chen, G. Y. J., Zhu, Q., and Yao, S. Q. (2002) Intein-mediated biotinylation of proteins and its application in a protein microarray, *J. Am. Chem. Soc. 124*, 8768−8769.
26. Tolbert, T. J., and Wong, C.-H. (2000) Intein-mediated synthesis of proteins containing carbohydrates and other molecular probes, *J. Am. Chem. Soc. 122*, 5421−5428.
27. Scopes, R. K. (1974) Measurement of protein by spectrophotometry at 205 nm, *Anal. Biochem. 59*, 277−282.
28. Milligan, J. F., and Uhlenbeck, O. C. (1989) Synthesis of small RNAs using T7 RNA polymerase, *Methods Enzymol. 180*, 51−62.
29. Liu, R., Barrick, J. E., Szostak, J. W., and Roberts, R. W. (2000) Optimized synthesis of RNA−protein fusions for *in vitro* protein selection, *Methods Enzymol. 318*, 268−293.
30. Barrick, J. E., Takahashi, T. T., Ren, J. S., Xia, T., and Roberts, R. W. (2001) Large libraries reveal diverse solutions to an RNA recognition problem, *Proc. Natl. Acad. Sci. U.S.A. 98*, 12374−12378.
31. Myszka, D. G. (2000) Kinetic, equilibrium, and thermodynamic analysis of macromolecular interactions with BIACORE, *Methods Enzymol. 323*, 325−340.
32. Myszka, D. G., and Morton, T. A. (1998) CLAMP: A biosensor kinetic data analysis program, *Trends Biochem. Sci. 23*, 149−150.
33. Fung, B. K.-K., and Nash, C. R. (1983) Characterization of transducin from bovine retinal rod outer segments. II. Evidence for distinct binding sites and conformational changes revealed by limited proteolysis with trypsin, *J. Biol. Chem. 258*, 10503−10510.
34. Hurley, J. B., Simon, M. I., Teplow, D. B., Robishaw, J. D., and Gilman, A. G. (1984) Homologies between signal transducing G proteins and ras gene products, *Science 226*, 860−862.
35. Kimple, R. J., Kimple, M. E., Betts, L., Sondek, J., and Siderovski, D. P. (2002) Structural determinants for GoLoco-induced inhibition of nucleotide release by Gα subunits, *Nature 416*, 878−881.
36. Peterson, Y. K., Hazard, S., Graber, S. G., and Lanier, S. M. (2002) Identification of structural features in the G-protein regulatory motif required for regulation of heterotrimeric G-proteins, *J. Biol. Chem. 277*, 6767−6770.
37. Higashijima, T., Ferguson, K. M., Sternweis, P. C., Ross, E. M., Smigel, M. D., and Gilman, A. G. (1987) The effect of activating ligands on the intrinsic fluorescence of guanine nucleotide-binding regulatory proteins, *J. Biol. Chem. 262*, 752−756.
38. McEwen, D. P., Gee, K. R., Kang, H. C., and Neubig, R. R. (2001) Fluorescent BODIPY-GTP analogs: Real-time measurement of nucleotide binding to G proteins, *Anal. Biochem. 291*, 109−117.
39. Clackson, T., and Wells, J. A. (1995) A hot spot of binding energy in a hormone-receptor interface, *Science 267*, 383−386.
40. Wall, M. A., Coleman, D. E., Lee, E., Iniguez-Lluhi, J. A., Posner, B. A., Gilman, A. G., and Sprang, S. R. (1995) The structure of the G protein heterotrimer $G_{i\alpha1}\beta_1\gamma_2$, *Cell 83*, 1047−1058.
41. Adhikari, A., and Sprang, S. R. (2003) Thermodynamic characterization of the binding of activator of G protein signaling 3 (AGS3) and peptides derived from AGS3 with $G\alpha_{i1}$, *J. Biol. Chem. 278*, 51825−51832.
42. Bourne, H. R. (1997) G proteins—The arginine finger strikes again, *Nature 389*, 673−674.
43. Coleman, D. E., Berghuis, A. M., Lee, E., Linder, M. E., Gilman, A. G., and Sprang, S. R. (1994) Structures of active conformations of $G_{i\alpha1}$ and the mechanism of GTP hydrolysis, *Science 265*, 1405−1412.
44. Scheffzek, K., Ahmadian, M. R., Kabsch, W., Wiesmüller, L., Lautwein, A., Schmitz, F., and Wittinghofer, A. (1997) The Ras−RasGAP complex: Structural basis for GTPase activation and its loss in oncogenic Ras mutants, *Science 277*, 333−338.
45. Tesmer, J. J. G., Berman, D. M., Gilman, A. G., and Sprang, S. R. (1997) Structure of RGS4 bound to AlF_4^--activated $G_{i\alpha1}$: Stabilization of the transition state for GTP hydrolysis, *Cell 89*, 251−261.
46. Li, S. W., and Roberts, R. W. (2003) A novel strategy for in vitro selection of peptide-drug conjugates, *Chem. Biol. 10*, 233−239.
47. Schatz, P. J. (1993) Use of peptide libraries to map the substrate specificity of a peptide modifying enzyme: A 13 residue consensus peptide specifies biotinylation in *Escherichia coli*, *Biotechnology 11*, 1138−1143.

BI0498398